University of New Hampshire

Magnus Effect on Cylindrical Airfoils

Zhangxi Feng, Simon Popecki, James Skinner

ME 646

Professor Todd Gross

5/9/2017

Table of Contents

Table of Figures

Table of Equations

Abstract

Our goal was to evaluate the Magnus Effect on cylindrical airfoils. Using the University of New Hampshire student wind tunnel we tested rotating cylinders (airfoils) at different mean wind velocities and rotational speeds. By keeping the velocity in the wind tunnel constant and changing the RPM of the cylinder we were able to track lift force trends. This test was completed for four different wind speeds - approximately: 12 m/s, 16 m/s, 20 m/s, 24 m/s; and three different cylinder radii 0.0290 m, 0.0419 m, and 0.0641 m. We ran an additional test on the smallest radius cylinder at constant RPM, and for a range of wind speeds between11 m/s and 30 m/s to more closely see the effect of average wind speed on lift. Theoretically, we expected to see a linear increase in lift as we increased wither wind speed or RPM, and exponential growth when increasing the cylinder radius. What actually occurred was an apparent plateau at our range of tested RPM and wind speeds with our size of cylinders. Despite seeing the expected increase in lift with radius, the total magnitude of lift was not nearly as close to our theoretical values. For our smallest cylinder we reach a Reynolds number as high as $1.128x10^5$, which is well above an appropriate Reynolds number for laminar flow- creating vortex shedding behind our cylinders reducing the experimental lift force.

Introduction

A spinning ball will drag more air to one side and create a force from the resulting pressure difference. For example, top spin drags more air to flow below the ball. According to Bernoulli's principle, faster air flow results in lower pressure, which causes the ball to curve downwards [1]. This is known as the Magnus effect. For cylinders, the Magnus lift force is found using the Kutta-Joukowski equation:

$$F_L = \mathrm{L}\rho u G \tag{1}$$

Where F_L is the Magnus lift force for a cylinder of length L in a fluid of density ρ flowing at a velocity u. The spin of the cylinder will create the vortex strength G found using the radius r of the cylinder and angular velocity ω in rad/s [2]:

$$G = 2\pi r^2 \omega \tag{2}$$

Combining equations 1 and 2 gives equation 3:

$$F_L = 2\pi r^2 \omega \rho u L \tag{3}$$

Equation 3 predicts a linear relationship between the angular velocity and the force, a linear relationship between the freestream velocity and the force, and a quadratic relationship between the cylinder radius and the force. This experiment aims to verify the accuracy of the Kutta-Joukouski equation at high rotational speeds by measuring the resulting lift forces on cylindrical airfoils of various radii at various wind speeds. Since the experiment involves fluid flow over the airfoil, the Reynolds number is also an important concept to check and verify the obtained results. The equation is given below:

$$Re = \frac{\rho u L}{\mu}$$

Where the Reynolds number Re is found using the fluid density, ρ, velocity, u, airfoil characteristic length, L, and fluid dynamic viscosity, μ.

Methods

Our test was conducted in a subsonic open return wind tunnel. The wind tunnel test section had a cross-sectional area of 18” by 18”. Two cylinders of diameters 2.28” and 3.3” were made from aluminum cans and a third cylinder of diameter 5.05” was made from a cardboard container. The aluminum cylinders had a plywood skeleton inside for stiffness – three wooden disks were spaced evenly inside the can. We press fit disks into the can with shims made from duct tape – this allowed the disks to fall into a balanced position after roughly 20 seconds of run time at 3,000 RPM, helping to balance the airfoils. One disk was in the middle of the can, and the other two disks were placed at the ends of the cylinder, and were attached to plain bearings driven by a Mega Motor ACn 16/15/4 brushless motor. The disks were balanced by drilling holes on opposite sides of missing material (low quality plywood). The motor was driven by a Thunderbird 18 Electronic Speed Controller connected to a Spektrum 2.4 GHz receiver. The cylinders had lengths of 5.125”, 6.938”, and 9” in order of increasing diameter. The cylinder was situated near the middle of the cross-section to minimize the effects of boundary layers from the walls. The setup was loaded in cantilever on a steel tube. The tube remained stationary while the airfoils rotated on it.

The steel tube was supported by an AFA2 force balance to measure lift force. The force balance had a resolution of 0.01 N and an accuracy of ± 0.2 N. We used a handheld tachometer to measure the RPM of the rotating cylinder with a resolution of 10 RPM and a fluctuation accuracy of about ± 200 RPM. Any dimension under 5” was measured with calipers. The diameter of the small and medium radius cylinders were measured to 0.001” or better. The lengths and the diameter of the large cylinder had a resolution of 0.05” (measured with machinist’s ruler). A pitot-static tube was used to measure the static and stagnation pressures in the wind tunnel, which were then used to calculate the wind speed. The speed was controlled by turning a dial controlling wind tunnel motor speed until the Pitot tube readings reached the desired level. The tube readings had a resolution of ± 0.05” of water (half the smallest tick spacing). We assumed the air density uncertainty from barometric pressure reading was negligible and the water density had an uncertainty of 0.05 kg/m^3, the errors for wind speeds were propagated to be:

$$E_u = u\frac{E_{Pdyn}}{2P_{dyn}}$$

Where P_{dyn} is the dynamic pressure found from the difference of static and stagnation pressures from the tube readings. The errors in the 4 wind speeds were found to be (12.0 ± 1.2) m/s (10%), (16.4 ± 0.9) m/s (5.4%), (19.8 ± 0.7) m/s (3.7%), and (24.0 ± 0.6) m/s (2.5%).

We conducted four trials for each cylinder at the each of the wind speeds. For each trial, the cylinders were rotated at three different RPMs. The large cylinder was run between 3500 RPM and 6000 RPM. The other two cylinders covered a range from 3000 RPM to 6000 RPM. Due to the accuracy of the tachometer and the fluctuating nature of the rotating cylinder, it was ineffective to maintain the same RPM across the trials. At the RPMs in the experiment, the expected forces from equation 3 range from 3.1 N at smallest diameter and slowest wind speed to 98 N at the largest diameter and fastest wind speed. 200 RPM difference would result in 4% to 6% error, which suggested the RPMs can be treated as equal when evaluating the effect of wind speed at constant RPM.

Results and Discussion

Figure 1**Error! Reference source not found.** below shows the decreasing lift force trend for increasing wind speed with the smallest diameter (Stella) cylinder at a constant 3760 RPM.

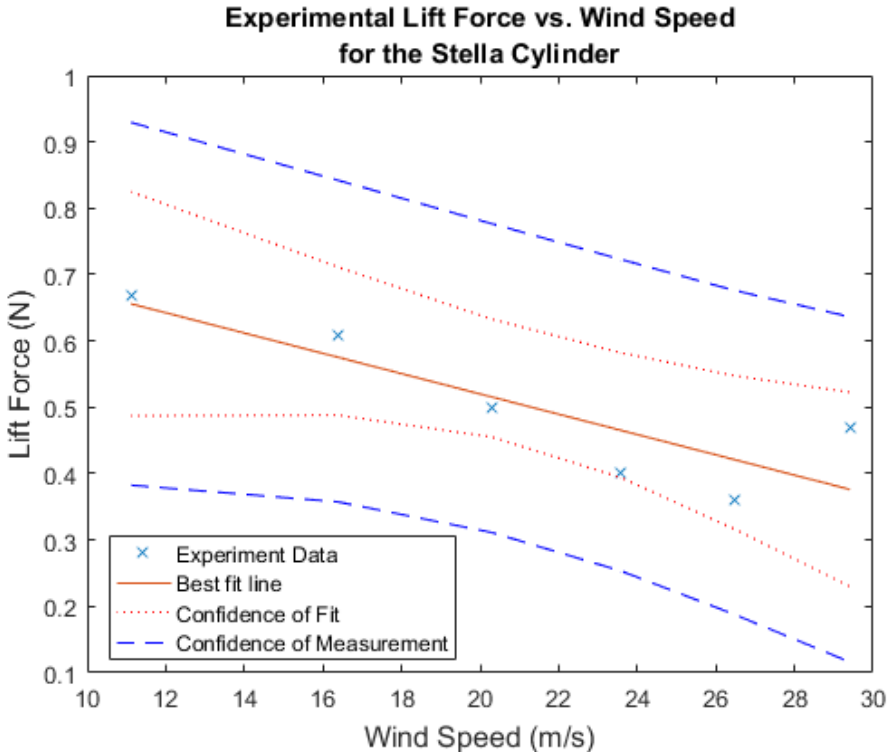

Figure 1 Smallest diameter cylinder measured lift force by increasing wind speed at constant RPM

This result is the opposite of the predicted positive linear relationship, showing the lift force decreased as the wind speed increased. The wide confidence intervals suggest that the experiment had a large uncertainty and was inconclusive in determining the effect of wind speed at a higher RPM on the lift force. The Reynolds numbers, independent of the cylinder's rotation, were found to be up to 1.12 x 10^5 (see tables Table A 5 to Table A 7). The Kármán vortex street is fully turbulent at this Reynolds number due to the flow separation caused by the wind speed [3]. A visualization of the vortex street is shown in figure 2:

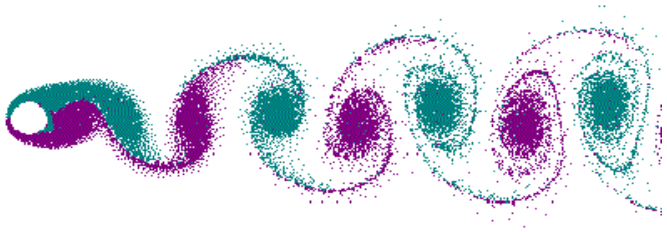

Figure 2 Visualization of the Kármán vortex streets for a stationary cylinder, from: https://disc.gsfc.nasa.gov/education-and-outreach/additional/science-focus/ocean-color/vonKarman_vortices.shtml

The Strouhal numbers for all trials were found to be the same at 0.198, which translates to vortex frequencies from18.53 Hz to 100.57 Hz (see tables A5 to A7 in Appendix A for tabulated values). The turbulent vortex street disrupted the pressure regions around the cylinder which also contributed to the large uncertainty in the measurement. Additionally, the rotation of the cylinder at 3760 RPM shifted the vortex streets towards the bottom and disrupted the bottom regions more than the top regions, possibly contributing to the decreasing lift.

The result of varying RPM at constant wind speed of 16.4 m/s for the smallest diameter cylinder is shown in figure 3 and the result for largest diameter (Quaker Oats) is shown in figure 4. The measured lift forces were significantly smaller than expected. The other trials produced similar results.

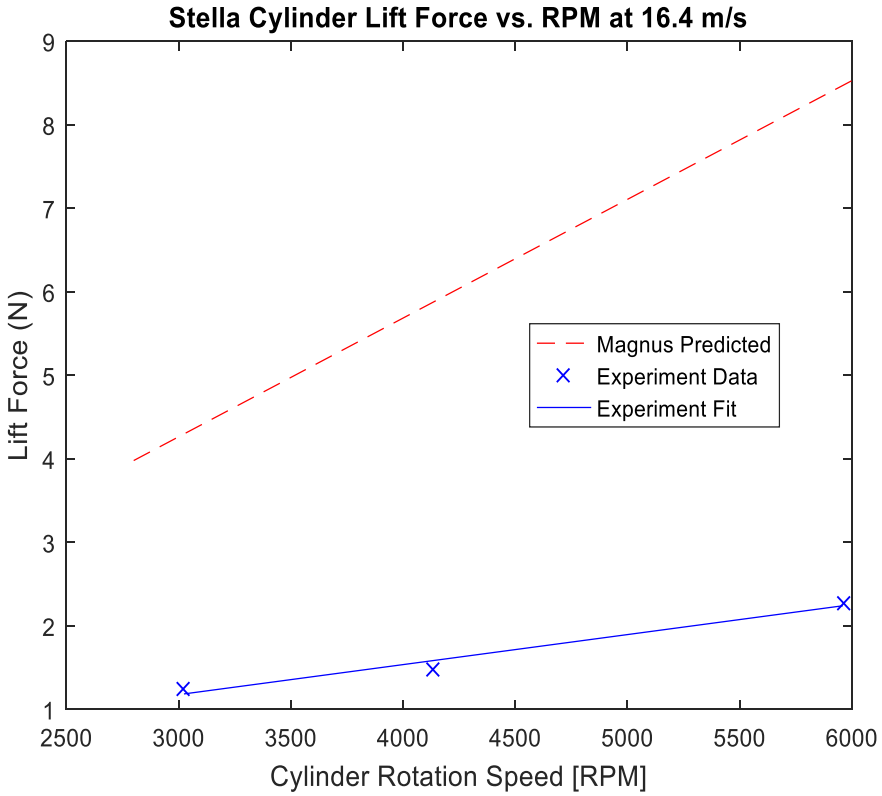

Figure 3 Smallest diameter cylinder measured vs predicted lift force at constant wind speed across the same RPM range

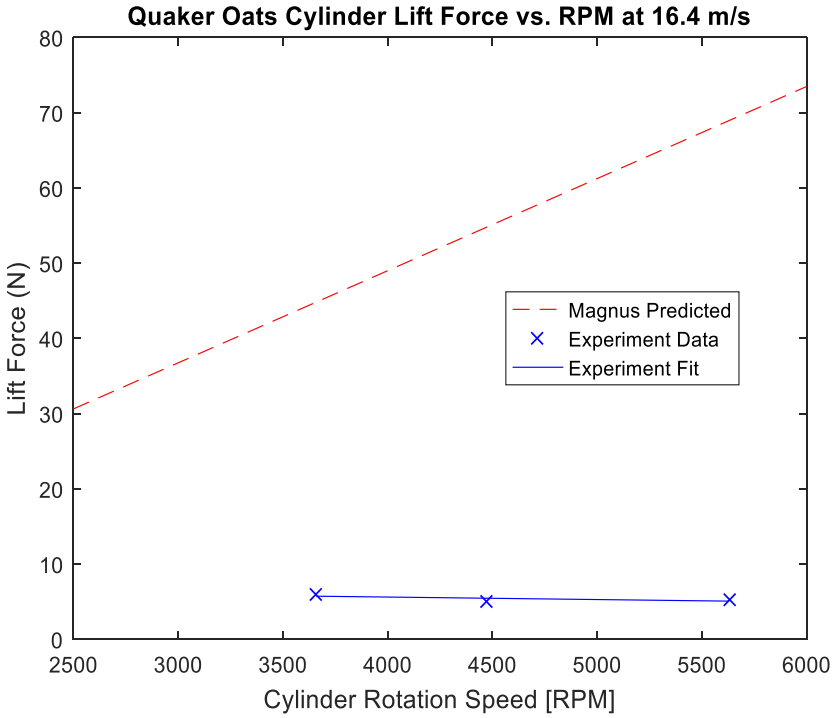

Figure 4 Largest diameter cylinder measured vs predicted lift force at constant wind speed across the same RPM range

figure 5 shows the results from a previous study of the effect of changing RPM on the lift coefficient at various Reynolds numbers and cylinder dimensions. Ω_0 is the tangential velocity found from RPM and the cylinder radius normalized by wind speed with the square symbols representing the case of largest cylinder span to diameter ratio, *A*, of 18.7 and a Reynolds number of 3.8 x 10^3, the circle and other illegible symbols representing the case of *A* ratio of 13.3 and various Reynolds numbers, and the dash line representing the smallest *A* ratio of 4.7 and a Reynolds number of 5.2 x 10^4. The figure suggests there exists a maximum coefficient of lift for each geometry and wind speed. Upon reaching a sufficiently high RPM, the lift coefficient begins to plateau. The maximum lift coefficient also decreases with smaller *A* ratio [4]. Our experiment can be best predicted from the dash line since our cylinders have *A* ratios of 2.24, 2.1, and 1.8

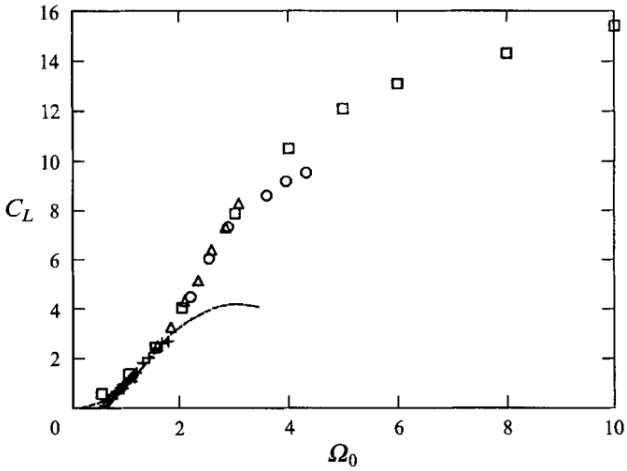

Figure 5 Lift coefficient versus normalized transverse velocities for various cylinders at various Reynolds numbers

from smallest to largest diameter respectively. This experiment's Ω_0 ranges from 0.5 to 3 with respect to slowest speed on smallest diameter to the fastest speed on the largest diameter.

The representative data below for the medium (Bud Heavy) cylinder at constant wind speed and a range of high RPM is shown in figure 6 below. The medium cylinder caused concern in the wind tunnel when conducting trials at the various constant wind speeds for the range of RPM. The AFA-2 force balance began to display erratic results in wide ranges which can be seen in figure 6, thus giving unreliable results for this cylinder size. The cylinder became unbalanced and caused concerning vibration on the experimental set-up which was causing the force balance to not operate properly. The medium cylinder became unbalanced as a result of the wooden disk in the center of the cylinder sliding down to one end of the airfoil while spinning inside the wind tunnel during testing. To adjust the center disk we would be required to remove the end caps of the cylinder and then reset all disks within the cylinder in the method previously described. We evaluated that disassembling the cylinder's supports could have led to more problems with the cylinder. We decided to continue our experiment, taking the data we had already collected, and continued on to our next cylinder.

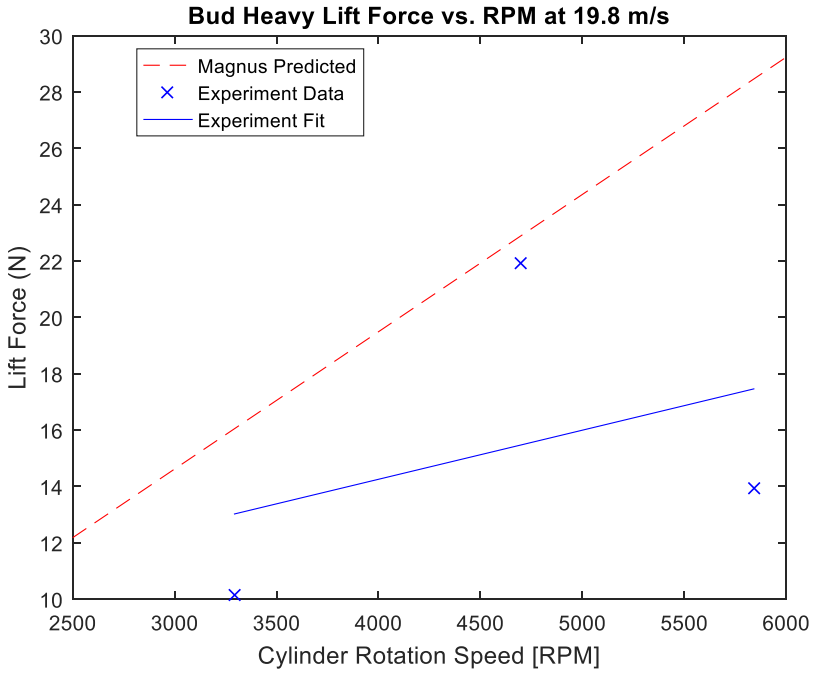

Figure 6 Medium sized cylinder measured vs predicted lift force at constant wind speed across the same RPM range

Summary and Conclusion

Paragraph 1: Purpose statement, result: measured lift force much lower (a percentage value) than predicted by formula

Paragraph 2: Major finding 1

Paragraph 3: Major finding 2

To test the validity Kutta-Joukowski lift equation (equation 1) at high rotational speeds we tested three different sized cylinders at different wind speeds and high rotational speeds. Based on this equation, you could theoretically produce an enormous amount of lift if you kept increasing any one of the factors from equation 3. Theoretically, we expected to see a linear increase in lift as we increased wind speed or RPM, and quadratic growth when increasing the cylinder radius.

Our experiment shows that at high rates of RPM and wind speed the difference between the theoretical and the obtained values are significant. After research we found that the wind speeds we were placing our model cylinders in was producing large Reynolds numbers that was producing a turbulence vortex behind the cylinder which disrupted the flow behind the cylinder. This disrupts the low pressure region above the cylinder and the high pressure region below the cylinder, because of this we assume the magnitude of pressure on the top and bottom are both increasing due to the alternating flow path beyond the cylinder as a result of the vortex.

References

[1] R. K. G. Kobes, "Bernoulli's Principle," 29 September 1999. [Online]. Available: http://theory.uwinnipeg.ca/mod_tech/node68.html. [Accessed 6 May 2017].

[2] N. Hall, "Lift of Rotating Cylinder," NASA, 5 May 2015. [Online]. Available: https://www.grc.nasa.gov/www/k-12/airplane/cyl.html. [Accessed 30 4 2017].

[3] S. Bengt, "Tubes, Crossflow over," Thermopedia, 16 March 2011. [Online]. Available: http://www.thermopedia.com/content/1216/. [Accessed 30 April 2017].

[4] P. a. D. P. Tokumaru, "The Lift of a Cylinder Executing Rotary Motions in a Uniform Flow," Cambridge University Press, Cambridge, UK, 1992.

Appendix A: Tables

Table A 1 Smallest diameter cylinder experiment data

Stella						
P1 (inH2O)	P2 (inH2O)	Delta h (m)	Wind Speed (m/s)	RPM	Lift (N)	Test
1.65	1.3	0.00889	12.00973309	3100	0.5	**TRIAL 1**
				4060	1.45	
				6000	1.96	
2	1.35	0.01651	16.36650742	3024	1.25	**TRIAL 2**
				4130	1.48	
				5960	2.28	
2.45	1.5	0.02413	19.78614266	2950	1.35	**TRIAL 3**
				3930	1.27	
				5950	2.31	
3	1.6	0.03556	24.01946618	2800	1.43	**TRIAL 4**
				4000	1.17	
				5870	2.11	

Table A 2 Medium diameter cylinder experiment data

Budweiser						
P1 (inH2O)	P2 (inH2O)	Delta h (m)	Wind Speed (m/s)	RPM	Lift (N)	
1.65	1.3	0.00889	12.00973309	3200	2.3	**TRIAL 1**
				4940	3.17	
				5800	1.65	
2	1.35	0.01651	16.36650742	*	*	**TRIAL 2***
				*	*	
				*	*	
2.45	1.5	0.02413	19.78614266	3291	10.13	**TRIAL 3**
				4700	21.92	
				5844	13.91	
3	1.6	0.03556	24.01946618	3100	10.25	**TRIAL 4**
				4860	13.11	
				5916	8.97	

Table A 3 Largest diameter cylinder experiment data

Oats						
P1 (inH2O)	P2 (inH2O)	Delta h (m)	Wind Speed (m/s)	RPM	Lift (N)	
1.65	1.3	0.00889	12.00973309	3720	3.72	**TRIAL 1**
				4560	3.14	
				5560	4.35	
2	1.35	0.01651	16.36650742	3660	6	**TRIAL 2**
				4470	4.97	
				5630	5.26	
2.45	1.5	0.02413	19.78614266	3675	8.42	**TRIAL 3**
				4050	7.25	
				5500	7.67	
3	1.6	0.03556	24.01946618	3000	10.6	**TRIAL 4**
				3160	15.5	
				5200	10.43	

Table A 4 Smallest diameter cylinder high wind speed experiment data

P1 (inH2O)	P2 (inH2O)	Delta h (m)	Wind Speed (m/s)	Lift (N)	RPM
1.5	1.2	0.00762	11.11885229	0.67	3760
2	1.35	0.01651	16.36650742	0.61	-
2.5	1.5	0.0254	20.30015404	0.5	-
3	1.65	0.03429	23.58664756	0.4	-
3.5	1.8	0.04318	26.46816261	0.36	-
4	1.9	0.05334	29.41771802	0.47	3760

Table A 5 Small diameter cylinder wind speed and corresponding Reynolds and Strouhal numbers

Stella			
Wind Speed (m/s)	**Reynolds Number**	**Strouhal Number**	**Vortex Frequency (Hz)**
12.0	4.60E+04	0.1979	41.04
16.4	6.27E+04	0.1979	55.94
19.8	7.58E+04	0.1979	67.63
20.0	9.21E+04	0.1980	82.11
29.4	1.13E+05	0.1980	100.57

Table A 6 Medium diameter cylinder wind speed and corresponding Reynolds and Strouhal numbers

Budweiser			
Wind Speed (m/s)	**Reynolds Number**	**Strouhal Number**	**Vortex Frequency (Hz)**
12.0	6.66E+04	0.1979	23.36
16.4	9.08E+04	0.1980	38.65
19.8	1.10E+05	0.1980	46.73
20.0	1.33E+05	0.1980	56.73

Table A 7 Largest diameter cylinder wind speed and corresponding Reynolds and Strouhal numbers

Quaker Oats			
Wind Speed (m/s)	**Reynolds Number**	**Strouhal Number**	**Vortex Frequency (Hz)**
12.0	1.02E+05	0.1980	18.53
16.4	1.39E+05	0.1980	25.26
19.8	1.68E+05	0.1980	30.54
20.0	2.04E+05	0.1980	37.07